

Selective Depletion Interactions in Mixtures of Rough and Smooth Silica Spheres

Marlous Kamp,[†] Michiel Hermes,[†] Carlos M. van Kats,[†] Daniela J. Kraft,[‡] Willem
K. Kegel,[¶] Marjolein Dijkstra,^{*,†} and Alfons van Blaaderen^{*,†}

[†]*Soft Condensed Matter, Debye Institute for Nanomaterials Science, Utrecht University,
Princetonplein 1, 3584 CC Utrecht, The Netherlands.*

[‡]*Soft Matter Physics, Huygens-Kamerlingh Onnes Lab, Leiden University, Niels Bohrweg
2, 2333 CA Leiden, The Netherlands.*

[¶]*Van't Hoff Laboratory for Physical & Colloid Chemistry, Debye Institute for
Nanomaterials Science, Utrecht University, Padualaan 8, 3584 CH, The Netherlands*

E-mail: m.dijkstra@uu.nl; a.vanblaaderen@uu.nl

Supporting Information

Supplementary Experimental Details

Materials

The following chemicals were used without further purification. From Sigma-Aldrich: rhodamine B isothiocyanate (RITC, mixed isomers), eosine isothiocyanate (EITC), 3-methacryloxypropyltrimethoxysilane (MPS, $\geq 98\%$), poly(allylamine hydrochloride) (PAH, $M_w \sim 15000$ a.m.u.). From Aldrich: cyclohexylchloride (CHC, 99%) and tetrabutylammonium chloride (TBAC). A steric stabilizer was synthesized by comb-grafting poly[12-hydroxystearic acid] (PHSA) onto a poly[methyl methacrylate] (PMMA) backbone through the method describe in Ref. 1. Polystyrene (565.500 g/mole) was used as a depletant.

TEM and SEM imaging were performed respectively on a TECNAI10 transmission electron microscope and a Nova 600 NanoLab from FEI company. Conductivity measurements were performed with a Scientifica model 627 conductometer.

Colloid synthesis

Rough silica particles were synthesized via a method resembling that in Ref. 2. Seed colloids for the rough particles were silica spheres with an FITC-labeled core prepared by Stöber synthesis as in Ref. 3. The particles had a diameter of $1.18 \pm 0.01 \mu\text{m}$ and polydispersity 2% as measured by TEM. These seed colloids were given a positive charge by adsorption of PAH molecules.⁴⁻⁷ In short, seed colloids were dispersed in a mixture of 20 mL water, 1.17 g NaCl and 0.06 g PAH. After stirring for at least 20 minutes, the particles were washed three times with water. Subsequently, slow sedimentation of these positively-charged seed colloids through a dispersion of small $130 \pm 4 \text{ nm}$ negatively charged EITC-labeled silica particles allowed the small particles to stick to the seed colloids. A clean-up procedure by three sedimentation redispersion steps was used to dispose of the excess small spheres. A thin $\sim 10 \text{ nm}$ Stöber silica layer was grown onto the final particles using seeded growth.⁸ The surface of the final rough particles was grafted with the silane coupling agent MPS to

make these colloids more hydrophobic for the intended solvent, and to allow for a similar environment for the steric comb-graft stabilizer PHSA-PMMA to be adsorbed onto as with PMMA particles.¹

Stöber silica particles grafted with the silane coupling agent MPS were used as smooth particles. These particles had a silica core of ~ 300 nm which was fluorescently labeled with FITC. The particles had a diameter of $1.24 \pm 0.01 \mu\text{m}$ (by TEM, polydispersity 2%) and 1320 nm in ethanol (by static light scattering, SLS⁸⁻¹⁰).

Confocal imaging

The rough particles contained an FITC-labeled core and EITC-labeled surface roughness. The emission maxima of FITC and EITC are close together (520 nm and 540 nm in ethanol¹¹) and the emission spectra overlap. Hence, the fluorescent signals of the core and the roughness could not be detected separately. The surface roughness can, however, be imaged employing scattering. Fig. S1 shows rough particles imaged with the SP8 confocal; the FITC cores were recorded using fluorescent mode and are depicted in green, while the surface roughness was recorded in scattering mode and is depicted in purple.

Zeta potential measurements

Zeta-potential measurements were performed on a Malvern ZetaSizer Nano. Although the Debye layer is determined by salt concentration alone, we wanted to verify whether the zeta potential was similar for rough and smooth particles. A zeta-potential measurement was performed on dilute dispersions of the smooth and the rough particles in a stock solution of CHC with salt and stabilizer. Both species of silica particles have a dye-free outer silica layer and similar (MPS) surface grafting. Differences in surface charge are thus not likely. The zeta potential was calculated from the electrophoretic mobility under assumption of the Schmoluchowski limit ($\lambda \ll R_{\text{colloid}}$). Fig. S2 shows the number of counts as a function of zeta-potential. The measured zeta potential of the smooth particles is -18 mV. The zeta

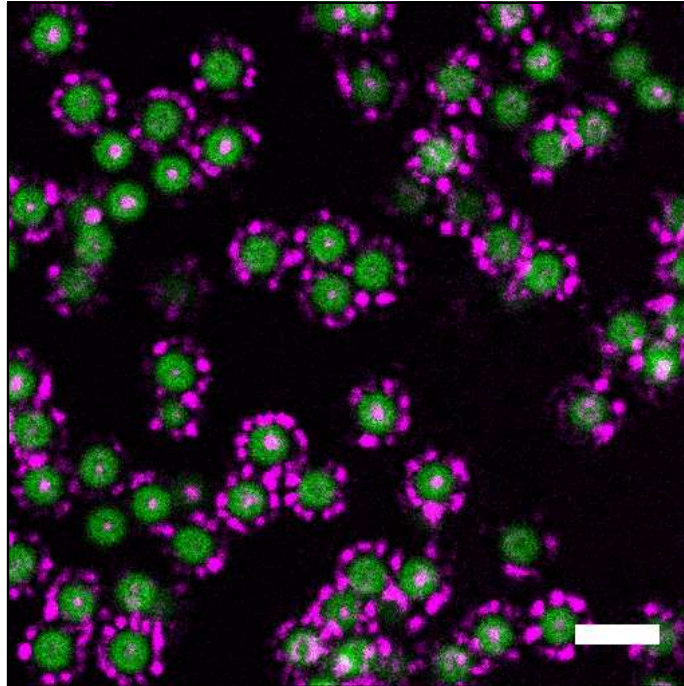


Figure S1: Confocal image of rough particles in CHC. The FITC-dyed cores were recorded in fluorescence mode (green), while the small particles at the surface were recorded using scattering mode (purple).

potential of the rough particles is centered about the same value, but it is very broad. These zeta potentials were deemed sufficiently close that the surfaces of the rough and smooth particles are deemed similar.

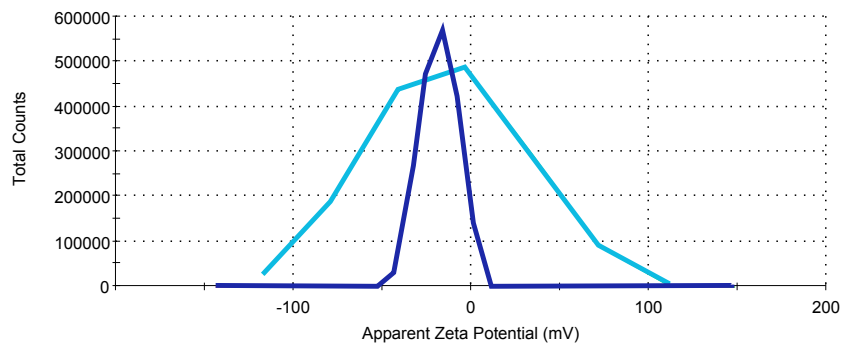


Figure S2: Zeta potentials calculated from the electrophoretic mobilities by the Smoluchowski equation for smooth particles (black line) and rough (grey line) particles in CHC saturated with TBAC and stabilized with PHSA.

Supplementary Simulation Details

Derivation of the effective Hamiltonian and depletion potential

We consider a system of N_C colloidal spheres at positions $\{\vec{R}\}$ with orientations $\{\hat{\omega}\}$ and N_p polymers at positions \vec{r}_j in a macroscopic volume V at temperature T . The system is described by the Hamiltonian H as described in *Methods*. We consider the system in the (N_c, V, z_p, T) ensemble, in which the fugacity $z_p = \Lambda_\nu^3 \exp(\beta\mu_p)$ of the polymer coils is fixed, with Λ_ν the thermal wavelength of species ν , and with μ_p the chemical potential of the polymers. The thermodynamic potential $F(N_c, V, z_p, T)$ of this ensemble can be written as

$$\exp(-\beta F) = \sum_{N_p=0}^{\infty} \frac{z_p^{N_p}}{N_c! \Lambda_c^{3N_c} N_p!} \text{Tr}_c \text{Tr}_p \exp[-\beta H], \quad (1)$$

where the trace Tr_c is short for the volume integral $\int_V d\vec{R}^{N_c} \int_\omega d\hat{\omega}^{N_c}$ over the coordinates and orientations of the coated particles, and similarly $\text{Tr}_p = \int_V d\vec{r}^{N_p}$. The effective Hamiltonian of the coated particles is written as

$$H^{\text{eff}} = H_{\text{cc}} - z_p V_f, \quad (2)$$

where $z_p V_f = z_p V_f(\{\vec{R}\}, \{\hat{\omega}\})$ is the negative of the grand potential of the fluid of ideal polymer coils in the static configuration of N_c coated colloids with coordinates \vec{R} and orientations $\hat{\omega}$. Here $V_f(\{\vec{R}\}, \{\hat{\omega}\})$ is the free volume of the polymers in the configuration of the colloids. Because of the ideal character of the polymer-polymer interactions it can be written explicitly as

$$V_f = \int_V d\vec{r} \exp\left[-\sum_{i=1}^{N_c} \beta \phi_{\text{cp}}(\vec{R}_i - \vec{r}_i, \hat{\omega}_i)\right]. \quad (3)$$

Non-vanishing contributions to V_f stem from those positions \vec{r} that are outside any of the N_c depletion shells. The shape of the free volume is highly irregular and non-connected. V_f can be decomposed, formally, into zero-colloid, one-colloid, two-colloid contributions, etc.,

by expanding it in terms of the colloid-polymer Mayer-function $f(\vec{R}_i - \vec{r}, \hat{\omega})$, which for the present model equals -1 for $\xi(\vec{R}_i - \vec{r}, \hat{\omega}) < 0$, and 0 otherwise. One finds

$$\begin{aligned} V_f &= \int_V d\vec{r} \prod_{i=1}^{N_c} (1 + f(\vec{R}_i - \vec{r}, \hat{\omega})) \\ &= V + \sum_{i=1}^{N_c} V_f^{(1)}(\vec{R}_i, \hat{\omega}_i) + \sum_{i < j}^{N_c} V_f^{(2)}(\vec{R}_i, \vec{R}_j, \hat{\omega}_i, \hat{\omega}_j) + \dots \end{aligned} \quad (4)$$

For $k \geq 1$, the k -colloid contribution reads

$$V_f^{(k)} = \int d\vec{r} \prod_{m=1}^k f(\vec{R}_{i_m} - \vec{r}, \hat{\omega}_{i_m}), \quad (5)$$

where only those positions \vec{r} give non-vanishing contributions where the depletion layers of (at least) k colloids overlap simultaneously.

We give explicit expressions for $V_f^{(k)}$ for $k = 1$ and 2 for equal-sized colloidal hard spheres with a smooth surface. It follows directly from Eq. 4 that the one-body contribution $V_f^{(1)} = -v_1$ with $v_1 = \pi\sigma_{\text{cp}}^3/6$ and $\sigma_{\text{cp}} = (\sigma_c + \sigma_p)/2$, which can be interpreted as the volume that is excluded for a polymer coil by a single colloid. $V_f^{(2)}(\vec{R}_i, \vec{R}_j)$ is the lens-shaped overlap volume of two spheres of radius σ_{cp} at separation $R_{ij} = |\vec{R}_i - \vec{R}_j|$. Note that $-z_p V_f^{(2)}(R_{ij}) \equiv \beta\phi_{\text{AO}}(R_{ij})$ is the well-known depletion potential of the AO model, which was derived by Asakura and Oosawa.¹² The effective pair potential $\phi^{\text{eff}}(R_{ij}) = \phi_{\text{cc}}(R_{ij}) + \phi_{\text{AO}}(R_{ij})$ reads

$$\beta\phi_{\text{eff}}(R_{ij}) = \begin{cases} \infty & \text{for } R_{ij} < \sigma_c, \\ -\frac{\pi\sigma_p^3 z_p (1+q)^3}{6q^3} \left[1 - \frac{3R_{ij}}{2(1+q)\sigma_c} + \frac{R_{ij}^3}{2(1+q)^3\sigma_c^2} \right] & \text{for } \sigma_c < R_{ij} < 2\sigma_{\text{cp}}, \\ 0 & \text{for } R_{ij} > 2\sigma_{\text{cp}}, \end{cases} \quad (6)$$

This Asakura-Oosawa pair potential describes an attractive well close to the surface of the colloid, whose depth increases linearly with increasing z_p . The range of the potential is given

by σ_p .

Similarly, an effective depletion potential is defined for our coated spheres, which depends explicitly on the orientation of the coated spheres

$$\beta\phi_{\text{eff}}(\vec{R}_{ij}, \hat{\omega}_i, \hat{\omega}_j) = \beta\phi_{\text{cc}}(\vec{R}_{ij}, \hat{\omega}_i, \hat{\omega}_j) - z_p \int_V d\vec{r} f(\vec{R}_i - \vec{r}, \hat{\omega}_i) f(\vec{R}_j - \vec{r}, \hat{\omega}_j). \quad (7)$$

The three- and more-body contributions $V_f^{(k)}$ with $k \leq 3$ will be zero when the radius of gyration of the polymer coils is sufficiently small compared to the size of the colloids. The mapping of the full Hamiltonian of the colloid-polymer mixture can then be mapped exactly onto an effective Hamiltonian with only effective pairwise additive interactions, since three colloidal spheres cannot simultaneously overlap with a polymer coil. If the relaxation of the orientation degrees of freedom is much faster than that of the translational degrees of freedom, and the coated particles are sufficiently isotropic, a further coarse-graining can be performed by integrating out the orientational degrees of freedom of the effective interactions. The orientation-averaged effective pair potential reads

$$\beta\phi_{\text{eff}}(R_{ij}) = -\log \left(\frac{1}{16\pi^2} \int_{\Omega} d\hat{\omega}_i \int_{\Omega} d\hat{\omega}_j \exp \left[-\beta\phi_{\text{cc}}(\vec{R}_{ij}, \hat{\omega}_i, \hat{\omega}_j) - z_p \int_V d\vec{r} f(\vec{R}_i - \vec{r}, \hat{\omega}_i) f(\vec{R}_j - \vec{r}, \hat{\omega}_j) \right] \right). \quad (8)$$

Since the integrals over the orientations of the particles cannot be solved directly, the orientational average is calculated by evaluating the integrand for many different random orientations. We have checked the convergence of our integrations.

Theoretical results on the effect of charge/steric stabilization

For charge-stabilized particles there is a lower bound on the polymer size that can generate depletion attraction: if the polymer is smaller than the thickness of this stabilization layer

the particles do not feel the attraction at all as the charge keeps the colloids apart. Since the polymer is expected to feel little or no effect of the surface charge of the particles, charge stabilization will effectively increase the distance to which the colloids can approach each other, while the polymers can still enter this exclusion layer. This has the same effect as roughness: it will decrease the effective attraction. To investigate the effect of a thin double layer on the interaction, we performed measurements of the pair potential between rough and smooth particles for exclusion layers of various sizes. We assumed that the exclusion layers are hard for other colloids but not for the polymers and the stabilization layer of other colloids.

For sterically stabilized systems the situation is different since the dense steric layer is expected to exclude the polymer as well. The steric stabilization will only increase the size of the colloids slightly. When the steric layer is smaller than the satellite particles that are used for the surface roughness, this should not have a significant effect. We have used the parameters of an experimental system which was synthesized by Kraft to obtain a quantitative estimate of the effect of the steric layer. In Fig. S3 we plot the effective pair potential between a smooth sphere with diameter $2.22\ \mu\text{m}$ and a sphere of $2.37\ \mu\text{m}$ covered with 900 small spheres with a diameter of $0.18\ \mu\text{m}$ and a total diameter of $2.8\text{-}3.0\ \mu\text{m}$. The polymer has a radius of gyration of $19\ \text{nm}$ resulting in an effective diameter of gyration of $38\ \text{nm}$. The effective attraction between the smooth spheres is again fixed at $6\ k_B T$, and the thickness of the stabilization layer is varied. The small attractive well that is visible for colloids without stabilization layer slowly disappears when the stabilization layer is increased in thickness, however, the fugacity of the polymers required also increases dramatically. (In fact, for a stabilization layer of $0.03\ \mu\text{m}$ the polymer concentration would be so high that the volume fraction would be well inside the semi-dilute regime. For these high volume fractions our assumption of ideal polymers fails. When the polymers are in the semi-dilute regime the range of the attraction will be less than expected from ideal polymers, which will increase the effect of the stabilization layer and the concentration of polymers required.¹³⁾ In short,

the stabilization does slightly increase the effect of the rough surface, however, the main effect of the stabilization layer is that it will increase the concentration of polymers required.

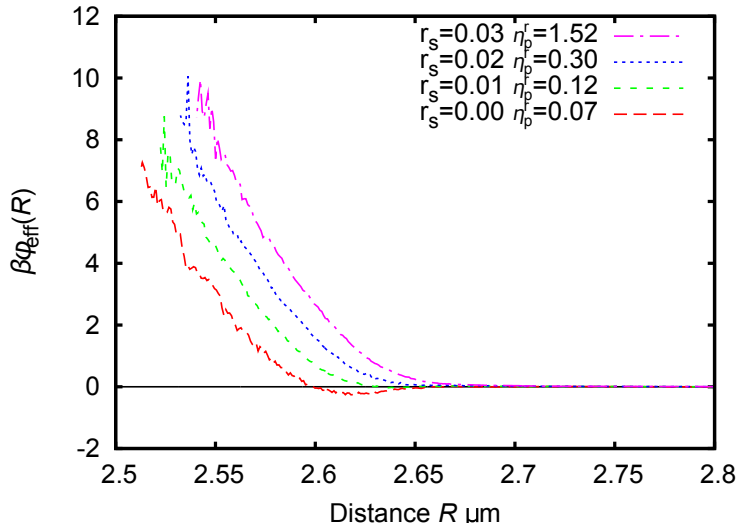


Figure S3: The effective pair potential between a smooth sphere with a diameter of $2.22 \mu\text{m}$ and a rough sphere with a diameter of $2.37 \mu\text{m}$ covered with 900 small spheres with diameter $\sigma_{\text{small}} = 0.18 \mu\text{m}$. The diameter of the polymers $\sigma_p = 38 \text{ nm}$. The thickness of the stabilization layer r_s and the polymer reservoir packing fraction η_p are varied as labeled. The polymer reservoir packing fraction is chosen such that the attraction between the smooth colloids is $6 k_B T$.

If the stabilization layer does not limit the size of the polymers the only remaining limitation is the roughness of the colloidal spheres. The surface roughness of the colloids should be smaller than twice the radius of gyration of the polymers otherwise this roughness reduces the attraction.

In the present experiments, the steric stabilizer consists of poly(12-hydroxystearic acid) (PHSA) comb-grafted onto a PMMA backbone. The PMMA backbone has affinity for the methacryloxypropyltrimethoxysilane-grafted silica, and the PHSA extends into the low-polar dispersion medium CHC. The maximum length of a chain of twelve carbons (this is the length of the chain up to the functional group which is grafted to the PMMA backbone, disregarding the bond angles in the carbon chain) is 1.7 nm . As a reasonable upper limit for the entire layer (MPS plus comb-grafted PHSA) we might estimate double this length: 3.4 nm . The steric layer thus adds less than 3% to the size of the satellite particles. In fact, the error is

on the order of the size measurement uncertainty. The steric stabilization layer increases the size of the central colloids by less than 0.3%.

Simulations regarding a rough particle and a hard wall

We investigated the onset of gelation for rough and smooth particles separately by testing the required polymer volume fraction needed for adhesion to a flat wall, as displayed in Fig. 6. While this experimental testing method gives a lower bound to the required polymer volume fraction, it is important to know to what degree the interaction potential between two spherical particles is different from that between a spherical particle and a flat wall. We approximated the case of a rough particle and a flat wall as the combination of a rough particle of diameter σ and a smooth particle of larger diameter. As the smooth sphere becomes bigger the potential approaches that of a smooth wall. The results are displayed in Fig. S4. The inset shows that the interaction potential between a rough and a smooth spheres of diameter 1 is nearly exactly the same as half of of that between a rough sphere and a sphere of diameter 50σ .

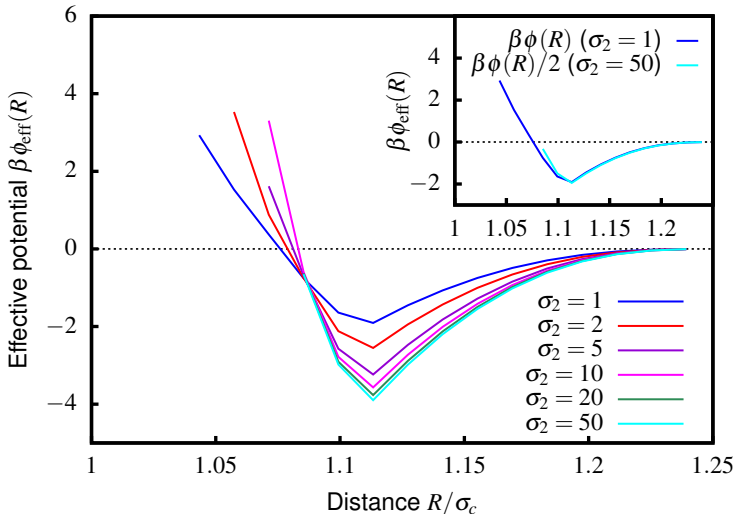


Figure S4: The pair potential between a rough sphere of diameter 1 and a smooth sphere of diameter σ_2 as labelled, derived from simulations.

A large body of work performed by Dijkstra and coworkers on depletion interactions

between particles and a wall can be found in literature (primarily Refs. 14–16 and related works 17–19). Complicated phase diagrams can arise in such systems including complete wetting and partial wetting regimes, and various layering transitions. Simulation evidence, including the effect of many-body effects (i.e. beyond a depletion pair potential picture) are presented in Refs.^{15,16} The main point that can be drawn from these works is that for depletion systems adsorption at the wall indeed occurs before bulk phase transition sets in. Indeed, a higher polymer concentration was required in our bulk experiments than the lower bounds found in Fig. 6.

Related to the work described in this paper where we investigate if significant attractions between smooth spheres can be realized by depletion effects while particles with rough surface are not yet driven to join in with either a phase separation and/or aggregation, Linse and Wennerström²⁰ investigated if such a window of inducing attractions exists for particles interacting with a short range attraction both amongst themselves and between a flat wall. Under the assumptions that the Derjaguin approximation is valid the attractions between a sphere and a wall are twice that of those between two spheres, however, entropic contributions make it not trivial if a window of attraction strengths exists where particle adsorption with the wall is appreciable, but bulk phase separation and/or aggregation is absent. These authors found that this window is present and in the present paper we actually used the attractions between the particle and a flat wall in a gravitational field to obtain experimentally an estimate of the attraction strengths.

Supplementary Video

The supplementary video displays a CSLM ‘z-stack’ (series of images taken along the direction of gravity) of a capillary filled with a dispersion of smooth (purple) and rough (green) spheres. The sample contains 2 wt.% PS. The smooth spheres have aggregated into a cluster while the rough spheres can move freely. The ‘z-stack’ was made immediately after plac-

ing the capillary onto the stage of the confocal microscope; not all rough particles have sedimented to the bottom glass yet. Moreover, some rough particles are trapped within aggregates of smooth particles. The ‘z-stack’ encompasses a height of $7.57\ \mu\text{m}$. Time between frames was 1.625 s and the video has a frame rate of 10 frames/s.

Supplementary SEM images

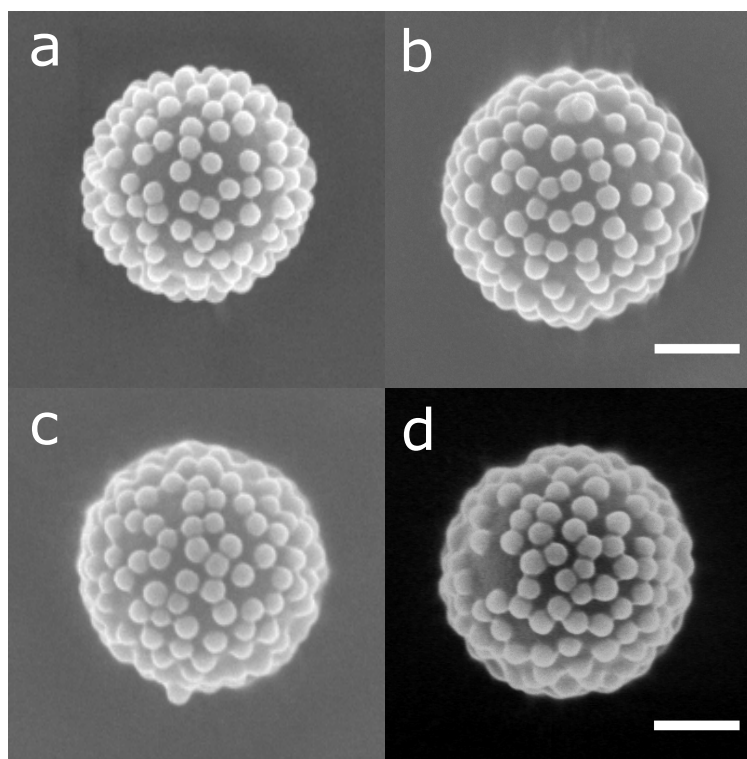


Figure S5: SEM micrographs of four different rough particles, showing the similarity of the surface morphologies. Scale bars denote 500 nm.

Supplementary References

- (1) Elsesser, M. T.; Hollingsworth, A. D. Revisiting the Synthesis of a Well-Known Comb-Graft Copolymer Stabilizer and Its Application to the Dispersion Polymerization of Poly(methyl methacrylate) in Organic Media. *Langmuir*, **2010**, *26*, 17989-17996.
- (2) Harley, S.; Thompson, D. W.; Vincent, B. The Adsorption of Small Particles onto Larger Particles of Opposite Charge: Direct Electron Microscope Studies. *Colloids and Surfaces* **1992**, *62*, 163-176.
- (3) van Blaaderen, A.; Vrij, A. Synthesis and Characterization of Colloidal Dispersions of Fluorescent, Monodisperse Silica Spheres. *Langmuir* **1992**, *8*, 2921-2931.
- (4) Decher, G. Fuzzy Nanoassemblies: Toward Layered Polymeric Multicomposites. *Science* **1997**, *277*, 1232-1237.
- (5) Lvov, Y.; Decher, G.; Moehwald, H. Assembly, Structural Characterization, and Thermal Behavior of Layer-by-Layer Deposited Ultrathin Films of Poly(Vinyl Sulfate) and Poly(Allylamine). *Langmuir* **1993**, *9*, 481-486.
- (6) Decher, G.; Schlenoff, J. B. Multilayer thin films: Sequential Assembly of Nanocomposite Materials. *Wiley-VCH Verlag GmbH & Co* **2012**.
- (7) Schmitt, J.; Decher, G.; Dressick, W. J.; Brandow, S. L.; Geer, R. E.; Shashidhar, R.; Calvert, J. M. Metal Nanoparticle/Polymer Superlattice Films: Fabrication and Control of Layer Structure. *Adv. Mater.* **1997**, *9*, 61-65.
- (8) van Blaaderen, A.; van Geest; Vrij, A. Monodisperse Colloidal Silica Spheres from Tetraalkoxysilanes: Particle Formation and Growth Mechanism. *J. Colloid Interface Sci.* **1992**, *154*, 481-501.
- (9) van Helden, A. K.; Vrij, A. Static Light Scattering of Concentrated Silica Dispersions in Apolar Solvents. *J. Colloid Interface Sci.* **1980**, *78*, 312-329.

- (10) Lehner, D.; Kellner, G.; Schnablegger, H.; Glatter, O. Static Light Scattering on Dense Colloidal Systems: New Instrumentation and Experimental Results. *J. Colloid Interface Sci.* **1998**, *201*, 34-47.
- (11) Meallier, P.; Guittonneau, S.; Emmelin, C.; Konstantinova, T. Photochemistry of Fluorescein and Eosin Derivatives. *Dyes and Pigm.* **1999**, *40*, 95-98.
- (12) Asakura, S.; Oosawa, F. Interaction between Particles Suspended in Solutions of Macromolecules. *J. Polymer Sci.* **1958**, *33*, 183-192.
- (13) Bolhuis, P. G.; Louis, A. A.; Hansen, J.-P. Influence of Polymer-Excluded Volume on the Phase-Behavior of Colloid-Polymer Mixtures. *Phys. Rev. Lett.* **2002**, *89*, 128302.
- (14) Brader, J. M.; Dijkstra, M.; Evans, R. Inhomogeneous Model Colloid-Polymer Mixtures: Adsorption at a Hard Wall. *Phys. Rev. E* **2001**, *63*, 041405
- (15) Dijkstra, M.; van Roij, R.; Roth, R.; Fortini, A. Entropic Wetting and Many-Body induced Layering in a Model Colloid-Polymer Mixture. *Phys. Rev. Lett.* **2002**, *89*, 208303.
- (16) Dijkstra, M.; van Roij, R. Effect of Many-Body Interactions on the Bulk and Interfacial Phase Behavior of a Model Colloid-Polymer Mixture. *Phys. Rev. E.* **2006**, *73*, 041404.
- (17) Evans, R.; Brader, J.M.; Roth, R.; Dijkstra, M.; Schmidt, M.; Löwen, H. Interfacial Properties of Model Colloid-Polymer Mixtures. *Philos. Trans. R. Soc., A* **2001**, *359*, 961-975.
- (18) Brader, J.M.; Evans, R.; Schmidt, M.; Löwen, H. Entropic Wetting and the Fluid-Fluid Interface of a Model Colloid-Polymer Mixture. *J. Phys. - Cond. Mat.* **2002**, *14*, L1-L8.
- (19) Brader, J. M.; Evans, R.; Schmidt, M. Statistical Mechanics of Inhomogeneous Model Colloid-Polymer Mixtures. *Mol. Phys.* **2003**, *101*, 3349-3384.

- (20) Linse, P.; Wennerström, H. Adsorption versus aggregation. Particles and surface of the same material. *Soft Matter* **2012**, *8*, 2486-2493.